AUTOMATIC SEGMENTATION OF CALCIFIED PLAQUE IN CAROTID ARTERIES

Jiehyun Kim[1] *Kevin Wang* [2] *Yu Sakai*[3] *Youxiang Zhu* [1]
Andrew C. Hu[3] *Huy Q. Phi*[4] *Nathan Arnett*[5] *Grace J. Wang* [3]
Brett L. Cucchiara[3] *Jae W. Song*[3] *Daniel Haehn*[1]

[1] University of Massachusetts Boston, Boston, MA, United States
[2] Net Health Systems Inc., Boston, MA, United States
[3]University of Pennsylvania, Philadelphia, PA, United States
[4] Drexel University College of Medicine, Philadelphia, PA, United States
[5]Brigham and Women's Hospital, Boston, MA, United States

ABSTRACT

Stroke remains a leading cause of death globally, with calcified plaque in the carotid artery being a significant risk factor. Evaluating the impact of calcified carotid plaque, particularly in patients with embolic stroke of undetermined source (ESUS), is critical yet challenging. Manual segmentation, essential for assessing stroke risk, is time-consuming, and conventional methods like 2D and 3D UNet often struggle with the small size of calcified plaques. Therefore, this paper introduces a two-step segmentation process. First, segments the carotid artery to narrow the search space and focus on the region of interest around the artery. Then, it segments the calcified plaque within that targeted region. This approach achieves an intersection over union (IoU) of 0.9412 for the 2D model and 0.8095 for the 3D model, outperforming the baseline methods that directly segment plaques. All developments are open source and publicly accessible on our GitHub: https://github.com/mpsych/CACTAS-AI.

***Index Terms*—** Calcified Plaque, Carotid Artery, Segmentation, UNet, CTA, Stroke

1. INTRODUCTION

Stroke is a leading global cause of death, accounting for 10% of all deaths worldwide [1]. The most common type, ischemic stroke, occurs when blood flow to the brain is blocked, often by plaque in the carotid artery. Some strokes are of unknown cause (ESUS: embolic strokes of undetermined source), despite thorough testing, and these patients have a 4-5% risk of having another stroke [2]. Imaging techniques, such as Computed Tomography Angiography (CTA) [3], help detect and assess these blockages, but analyzing them manually is time-consuming.

We study automatic methods that segment carotid artery plaque in CTA images, specifically targeting ESUS data. CarotidNet and CA-UNet segment the carotid artery using a 3D UNet architecture [4, 5], but both methods require carotid artery annotations. CarotidAnalyzer also utilizes a 3D UNet to segment the lumen and plaque [6], though it requires heavy user interaction. Zhai et al. employed a 3D UNet to segment carotid artery regions and a ResUNet to segment and classify plaques [7]. While this approach is fully automatic, it still requires annotation files for both the carotid artery and plaques to train the model. To the best of our knowledge, no studies have focused on ESUS cases. Furthermore, obtaining ground truth for both the carotid artery and plaque is time-consuming. To address this, we propose a two-step segmentation process (Fig. 1). First, we segment the carotid artery for each patient in the CTA image. We then use this segmentation to mask the image and focus specifically on the area around the carotid artery for plaque detection. This pipeline then informs a machine learning model that automatically identifies carotid artery plaque in CTA images.

2. DATASET

The dataset is part of the Penn Stroke Registry, a registry of acute ischemic stroke patients. The ESUS cases were identified to retrieve head and neck CTA images, which were then annotated for calcified plaques by medical professionals. The datasets have a resolution of 512 by 512 pixels, with varying sizes along the z-axis. We utilize three independent CTA neck imaging data sets: ESUS, CEA, and CAS. First, we used a dataset of patients with ESUS (N=70). Second, we acquired a second dataset from the Penn Vascular Quality Initiative comprised of patients who underwent carotid endarterectomy (CEA, N=27) or carotid stenting (CAS, N=17) for carotid plaque disease. All cases had calcified carotid plaques manually segmented by two independent annotators and proofed by an expert radiologist.

ESUS. The calcified plaques in Embolic strokes of undetermined source (ESUS) cases are relatively small size with mild stenosis, which is $\leq 50\%$ lumenal stenosis.

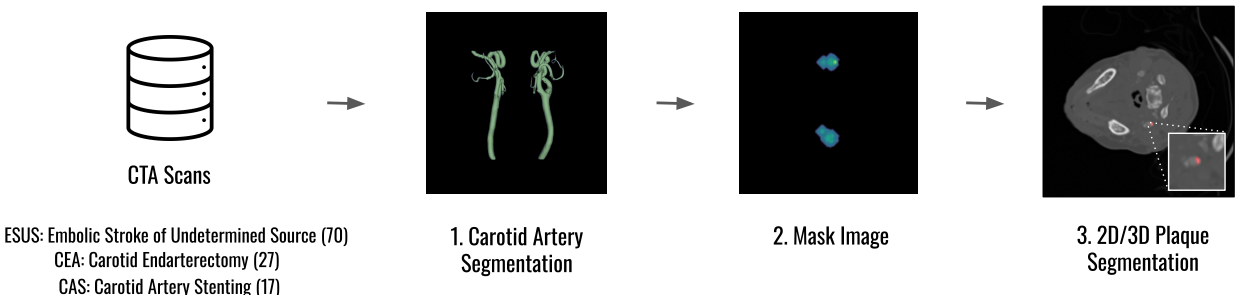

Fig. 1. For each CTA scan, the first step is creating a carotid artery mask, followed by applying the mask to the original image. The final step is to train the 2D/3D U-Net model to segment the calcified plaque.

CEA, CAS. The calcified plaques in carotid endarterectomy (CEA) and carotid artery stenting (CAS) cases are larger, likely contributing to severe >70% lumenal stenosis.

3. CAROTID ARTERY SEGMENTATION

3.1. Method

We obtained ground truth annotations from medical professionals using PlaqueIQ and used TotalSegmentator to segment the carotid artery.

PlaqueIQ. PlaqueIQ is an FDA-cleared computed tomography angiography (CTA) algorithm that objectively quantifies plaque composition, validated against histology, the gold standard for plaque characterization recognized by pathologists, a semi-automatic tool.

TotalSegmentator. The TotalSegmentator is a deep learning-based segmentation model designed to automatically segment all major anatomical structures on body CT scans [8].

Mask Creation. Utilizing the TotalSegmentator, we segment the common carotid artery (CCA). Although some sections were fully segmented, most areas remained partially segmented. Additionally, plaque segmentation is typically located around the carotid bifurcation, which is higher than the common carotid artery and closer to the internal carotid artery (ICA) and external carotid artery (ECA).

Using the TotalSegmentator output as initial seeds, we analyzed carotid artery intensity values and calculated a threshold based on the mean intensity. Specifically, we defined the range by subtracting 50 and adding 200 to the mean. The upper bound of +200 was chosen after observing typical intensity variations within this range, while subtracting 50 for the lower bound improved segmentation accuracy, likely enhancing boundary outline. Thus, we set threshold ranges of -50 and +200. The images were then cropped around the carotid artery, guided by vertebrae segmentation from TotalSegmentator. As carotid length varies by patient, we determined the cropping range based on vertebral levels C3 to C5 [9]. Finally, we applied a region-growing technique to produce the carotid artery mask.

3.2. Evaluation

We obtained output from the TotalSegmentator and the post-processed mask, but neither represented the ground truth segmentation created by medical professionals. We acquired ground truth segmentation using PlaqueIQ, which segments the carotid artery and identifies five different types of plaques within the artery. We aim to develop a fully automatic carotid artery segmentation process that achieves reliable accuracy while reducing segmentation time. Therefore, we evaluated and compared the outputs of TotalSegmentator, PlaqueIQ, and the post-processed TotalSegmentator mask in Table 1, focusing on accuracy, processing time, and operational efficiency.

Accuracy. The accuracy was assessed by bounding box comparison for a rough evaluation, as our primary focus was ensuring the plaque was included. If the plaque's bounding box was inside the carotid artery's bounding box, it was counted as an accurate mask; otherwise, it was not. None of the TotalSegmentator outputs included the entire plaque. PlaqueIQ, however, captured all plaques, as it was guided by medical professionals who proofed the semiautomated tool's segmentation output. The TotalSegmentator with post-processed mask successfully captured 90% of plaques, making it highly reliable.

Timing. The time was measured based on processing 70 datasets. TotalSegmentator took approximately 1 minute per both left and right carotid artery, totaling around 70 minutes. On the other hand, PlaqueIQ required variable amounts of time depending on the complexity of the course of the artery and plaque compositional complexity. For the carotid artery and plaque segmentation, we selected the minimal processing time of one hour for each carotid artery—either left or right—per patient, resulting in approximately 5 days and 20 hours. The TotalSegmentator with post-processing took about 70 minutes for the initial segmentation and an additional post-processing time, leading to a total of 5 hours and 47 minutes, which is significantly less time than PlaqueIQ.

Mode. TotalSegmentator and TotalSegmentator+Postproc are fully automatic tools, whereas PlaqueIQ is a semi-automatic

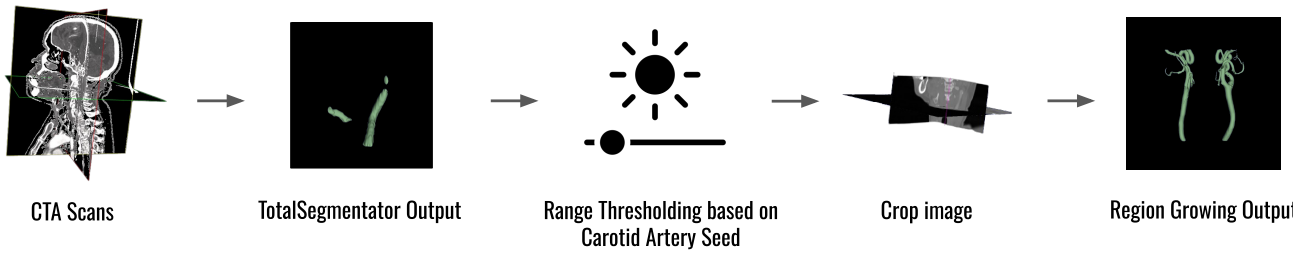

Fig. 2. For each CTA scan, we use the output of TotalSegmentator as a seed for intensity thresholding followed by cropping the volume and region growing to create complete carotid artery masks.

Table 1. For carotid artery segmentation, we compare TotalSegmentator (TS), PlaqueIQ, and TS + postprocessing, which offers automatic processing and high accuracy in reasonable time.

	Total Segmentator	**PlaqueIQ**	**TS + Postproc**
Accuracy [%]	0	100	90
Time [min]	70	8400	347
Mode	Automatic	Semi-Automatic	Automatic

tool. For a more thorough comparison, we trained a 2D UNet for carotid artery segmentation and compared the results with the ground truth provided by PlaqueIQ. Intersection over Union (IoU) is used as an evaluation metric, which is an area of overlap over an area of a union. After applying a threshold value of 0.5, we achieved an IoU score of 0.8416, indicating high accuracy.

4. PLAQUE SEGMENTATION

4.1. Data preprocessing

The ESUS dataset was divided into training and testing subsets randomly using an 8:2 ratio for the ESUS-only experiment. Similarly, for the ESUS+CEA+CAS experiment, all datasets (ESUS, CEA, and CAS) were combined and split in the same 8:2 ratio for training and testing. In both experiments, the training subset was further divided into training and validation sets, again using an 8:2 ratio within the training subset. For the 2D UNet, the images were normalized and sliced along the z-axis for further processing. We masked the CTA images with carotid artery segmentation to emphasize the carotid artery region. These focused images were paired with the corresponding plaque segmentation labels, collectively serving as the image and label input. In the 3D UNet, the images were masked and cropped based on the carotid artery segmentation. We use random rotation, scaling, shearing, and multiplane transformations for data augmentation techniques, and the cropped, masked images and plaque labels were used in the 3D UNet model for training.

4.2. 2D and 3D UNet Training

The UNet is a widely used deep learning model in biomedical image segmentation [10]. Although there are numerous state-of-the-art pipelines, including nnUNet [11] and the Swin Transformer-based SwinUNetr [12], UNet remains a strong, simpler, and commonly used baseline. Furthermore, because the ESUS dataset has not yet been tested with any model, we selected UNet as our baseline for the present study.
2D UNet. To facilitate the training of this model, the Adam optimizer is employed efficiency, leveraging the first and second-order momentum to reduce velocity and enhance accuracy and efficiency [13]. The learning rate is held constant at 0.001. Sigmoid is the activation function [14], and binary cross-entropy is the loss function [15]. Each model was trained for 200 epochs with a batch size of 16.
3D UNet. We used the same optimizer, learning rate, and activation function; however, we employed the dice loss function and reduced the batch size to 2 due to memory limitations.
Evaluation Metric: Intersection-over-Union (IoU). IoU quantifies the intersection area divided by the union area. The IoU threshold represents the proportion of the true bounding box area to the predicted bounding box area.

Table 2. Plaque segmentation performance metrics, using Intersection over Union (IoU), of 2D UNet and 3D UNet on different datasets. ALL indicate ESUS, CEA, and CAS data. The higher, the better.

Run Type	Dataset	2D UNet	3D UNet
Best Performance	ESUS	0.9412	0.8095
	ALL	0.3920	0.6840
Cross-Validation	ESUS	0.7114	0.6230
	ALL	0.2361	0.4976

Plaque Segmentation. We conducted two different experiments. As shown in Table 2, we first tested the ESUS dataset exclusively. For the 2D UNet, we achieved an IoU of 0.9412, while the 3D UNet resulted in an IoU of 0.8095. The result

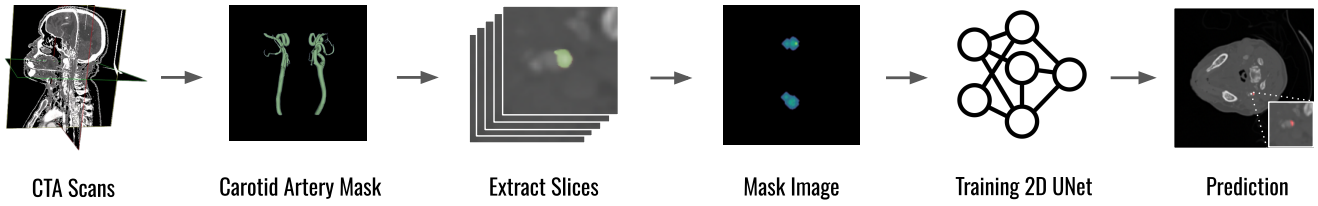

Fig. 3. To train a 2D UNet for plaque segmentation, we use the carotid artery masks from Step 1 from Fig. 2, extract 2D Slices, and then mask the image based on the artery label.

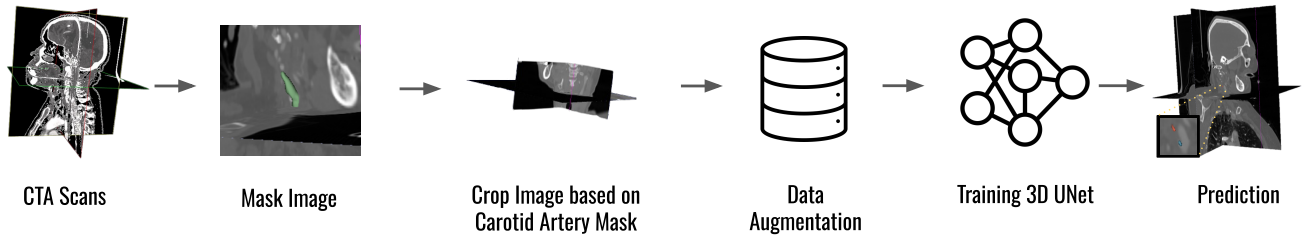

Fig. 4. To train a 3D U-Net for plaque segmentation, we first mask the images, then crop them based on the carotid artery region, and finally apply data augmentation to the dataset.

images are shown in Fig 3 and Fig 4 Prediction step. Both models segmented the calcified plaque effectively, but the 2D UNet demonstrated better performance.

Next, we applied the model to different datasets—CEA and CAS—to test the generalizability of our models. In this experiment, the 2D UNet achieved an IoU of 0.3920, whereas the 3D UNet yielded a significantly higher IoU of 0.6840. This suggests that the 3D UNet performs better across diverse datasets, indicating better generalization capability.

Ablation Study. We initially applied a conventional approach to plaque segmentation, using 2D and 3D UNet on CTA images with plaque annotations. This initial segmentation was performed without focusing on the carotid artery region, aiming to segment the plaques directly from the full CTA images. Intersection over Union (IoU) scores were 0.0283 for the 2D UNet and 0.0433 for the 3D UNet. The high volume of information in the CTA scans and the relatively small size of the plaques can explain low performance.

4.3. Cross Validation

For the 2D UNet, five-fold cross-validation was used because the dataset contained 28,162 slices (ESUS+CEA+CAS data), making Leave-One-Out Cross-Validation (LOOCV) computationally impractical. In contrast, LOOCV was chosen for the 3D UNet, which only contained 114 volumes, due to the smaller dataset size. For the 3D UNet, we saved weights for each training and compared each weight to ground truth for testing.

Table 2 presents the cross-validation results for both 2D and 3D UNet models. For the ESUS dataset, the 2D UNet achieved an IoU of 0.7114, while the 3D UNet obtained an IoU of 0.6230. When applied to the full dataset, which includes ESUS, CEA, and CAS cases, the 2D UNet recorded a lower IoU of 0.2361, and the 3D UNet recorded an IoU of 0.4976, indicating that neither model performed effectively when applied to the entire dataset. This performance decrease is likely due to differences in plaque size—smaller plaques in ESUS and larger plaques in CEA and CAS—as well as dataset imbalance, with a larger number of ESUS samples (N=70) compared to CEA (N=27) and CAS (N=17).

5. CONCLUSION

In this paper, we present a two-step process for segmenting the carotid artery followed by the segmentation of calcified plaque. Our study demonstrates that the 2D UNet model performs better than the 3D UNet, specifically on the ESUS dataset, indicating its suitability for tasks involving small, specific datasets. However, when considering the broader context and evaluating across all datasets, the 3D UNet performs better, effectively segmenting calcified plaques in diverse datasets. This suggests that while the 2D UNet is preferable for targeted use cases such as ESUS, the 3D UNet offers flexibility for different datasets, making it more suitable for more extensive datasets. Additionally, future research will focus on optimizing both models for different dataset characteristics, thereby improving performance in various clinical scenarios. This work is fully open source, with resources provided for reproducibility.

6. COMPLIANCE WITH ETHICAL STANDARDS

Datasets were acquired from the Penn Stroke Registry and shared under a data use agreement. The data was fully de-identified, and the researchers were not provided with personally identifiable information.

7. REFERENCES

[1] World Health Organization, "The top 10 causes of death," 2020, Accessed: 2020-12-09.

[2] George Ntaios, "Embolic stroke of undetermined source: Jacc review topic of the week," *Journal of the American College of Cardiology*, vol. 75, no. 3, pp. 333–340, 2020.

[3] DRJ Owen, AC Lindsay, RP Choudhury, and ZA Fayad, "Imaging of atherosclerosis," *Annual review of medicine*, vol. 62, no. 1, pp. 25–40, 2011.

[4] Tianshu Zhou, Tao Tan, Xiaoyan Pan, Hui Tang, and Jingsong Li, "Fully automatic deep learning trained on limited data for carotid artery segmentation from large image volumes," *Quantitative Imaging in Medicine and Surgery*, vol. 11, no. 1, pp. 67, 2021.

[5] Yuqi Zhang, Mengbo Yu, Chao Tong, Yanqing Zhao, and Jintao Han, "Ca-unet segmentation makes a good ischemic stroke risk prediction," *Interdisciplinary Sciences: Computational Life Sciences*, vol. 16, no. 1, pp. 58–72, 2024.

[6] Pepe Eulzer, F von Deylen, W-C Hsu, Ralph Wickenhöfer, Carsten M Klingner, and Kai Lawonn, "A fully integrated pipeline for visual carotid morphology analysis," in *Computer Graphics Forum*. Wiley Online Library, 2023, vol. 42, pp. 25–37.

[7] Duchang Zhai, Rong Liu, Yan Liu, Hongkun Yin, Wen Tang, Junlin Yang, Kefu Liu, Guohua Fan, Shenghong Ju, and Wu Cai, "Deep learning-based fully automatic screening of carotid artery plaques in computed tomography angiography: a multicenter study," *Clinical Radiology*, 2024.

[8] Jakob Wasserthal, Hanns-Christian Breit, Manfred T Meyer, Maurice Pradella, Daniel Hinck, Alexander W Sauter, Tobias Heye, Daniel T Boll, Joshy Cyriac, Shan Yang, et al., "Totalsegmentator: robust segmentation of 104 anatomic structures in ct images," *Radiology: Artificial Intelligence*, vol. 5, no. 5, 2023.

[9] Mihaela Daniela Manta, Mugurel Constantin Rusu, Sorin Hostiuc, Răzvan Costin Tudose, Bogdan Adrian Manta, and Adelina Maria Jianu, "The vertical topography of the carotid bifurcation–original study and review," *Surgical and Radiologic Anatomy*, vol. 46, no. 8, pp. 1253–1263, 2024.

[10] Olaf Ronneberger, Philipp Fischer, and Thomas Brox, "U-net: Convolutional networks for biomedical image segmentation," in *Medical Image Computing and Computer-Assisted Intervention–MICCAI 2015: 18th International Conference, Munich, Germany, October 5-9, 2015, Proceedings, Part III 18*. Springer, 2015, pp. 234–241.

[11] Fabian Isensee, Paul F Jaeger, Simon AA Kohl, Jens Petersen, and Klaus H Maier-Hein, "nnu-net: a self-configuring method for deep learning-based biomedical image segmentation," *Nature methods*, vol. 18, no. 2, pp. 203–211, 2021.

[12] Ali Hatamizadeh, Vishwesh Nath, Yucheng Tang, Dong Yang, Holger R Roth, and Daguang Xu, "Swin unetr: Swin transformers for semantic segmentation of brain tumors in mri images," in *International MICCAI brainlesion workshop*. Springer, 2021, pp. 272–284.

[13] Diederik P. Kingma and Jimmy Ba, "Adam: A method for stochastic optimization," 2014.

[14] Shiv Ram Dubey, Satish Kumar Singh, and Bidyut Baran Chaudhuri, "Activation functions in deep learning: A comprehensive survey and benchmark," 2021.

[15] Zhilu Zhang and Mert R. Sabuncu, "Generalized cross entropy loss for training deep neural networks with noisy labels," 2018.